Sigma Bond Activation by Cooperative Interaction with ns^2 Atoms: $B^+ + nH_2$

Stephanie B. Sharp and Gregory I. Gellene*

Contribution from the Department of Chemistry and Biochemistry, Texas Tech University, Lubbock, Texas 79409-1061

Received January 8, 1998. Revised Manuscript Received April 13, 1998

Abstract: The reactions of $B^+ + nH_2$ to produce $BH_2^+(H_2)_{n-1}$ have been studied by high-level ab initio techniques. The reaction mechanism and associated activation energy is found to depend dramatically on the number of H_2 molecules present. For $n = 1$, the reaction proceeds stepwise: first breaking the H_2 bond and forming one BH bond followed by forming the second BH bond. This process has an activation energy of about 57 kcal/mol. For $n = 2$, the reaction proceeds via a pericyclic mechanism though a planar cyclic transition state where two H_2 bonds are broken while simultaneously two BH bonds and one new H_2 bond are formed. The activation energy for this process decreases dramatically from the $n = 1$ value to only about 11 kcal/mol. For $n = 3$, the reaction proceeds through a true insertion mechanism; however, the actual insertion occurs late in the reaction after over 75% of the exothermicity has been realized. The addition of the third H_2 molecule decreases the activation energy to only about 3.4 kcal/mol. For $n = 4$, the reaction mechanism is essentially identical to that of the $n = 3$ case. However, the fourth H_2 causes the activation energy to increase by about 2 kcal/mol relative to the $n = 3$ case because the additional H_2 molecule causes one of the other three H_2 molecules to be slightly further away from the boron ion in the transition state geometry. The computational results are compared with the experimental results of Kemper, Bushnell, Weis, and Bowers (*J. Am Chem. Soc.* ***1998***, *120*, xxxx) and are in full agreement with the experimental conclusion that the $n = 3$ electrostatic cluster ion is the most reactive. On the basis of a comparison of experimentally determined magnitude and isotopic dependence of the activation energies with the computed adiabatic reaction barriers, it is suggested that the observed reaction rate may be dominated by a nonclassical tunneling contribution.

Introduction

The reaction of B^+ (^1S_g) with H_2 ($^1\Sigma_g^+$) to produce the centrosymmetric ($D_{\infty h}$) covalently bound HBH^+ ($^1\Sigma_g^+$) ion is exothermic by more than 50 kcal/mol. Nevertheless, the gas-phase reaction proceeds inefficiently due to the presence of a large activation energy. The origin of the reaction barrier has been discussed previously by Nichols *et al.*[1] in the context of guided ion beam[2,3] and other experimental studies[4] of BH^+ formation from B^+/H_2 collisions and is straightforward to understand. The analysis is simplified by considering a constrained C_{2v} geometry for the reaction coordinate (Figure 1). At large B^+/H_2 separation a $^1A_1$ electronic ground state of the electrostatic complex arises from the four valence electrons adopting a $(2a_1)^2(3a_1)^2$ electron configuration. The lower energy orbital has no nodes between boron and H_2 and the higher energy orbital has one such node lying parallel to the H−H axis. Alternatively, at small B^+/H_2 separation a $^1A_1$ electronic ground state of the covalent molecular ion arises from the four valence electrons adopting a $(2a_1)^2(1b_2)^2$ electron configuration. As was the case at large separation, the lower energy orbital has no nodes between boron and hydrogen. However, the node of the higher energy orbital now lies perpendicular to the H−H axis. Thus, although the electronic state is always labeled as $^1A_1$ in C_{2v} symmetry, the $(3a_1)^2$ occupancy of large separation ground state correlates with an excited electronic state at small separation and an energetic barrier to reaction ensues.

Very recently, Kemper, Bushnell, Weis, and Bowers[5] (KBWB) reported that the electrostatic complexation of the B^+ ion to three H_2 molecules caused the activation energy for HBH^+ formation to decrease to almost zero. Considering that the electrostatic binding energy of each H_2 molecule is expected to be only about 2−4 kcal/mol, this dramatic activation energy decrease could not be attributed simply to the energetic effects of H_2 clustering on B^+. A cluster assisted mechanism for σ bond activation has been observed previously for the transition metal systems Sc^+/H_2 (ref 6) and Ti^+/CH_4 (ref 7). However, in those cases the explanation involved an energetic reordering of the low-lying electronic states of the metal ion upon complexation which cannot be the case for the B^+ ion. Nevertheless, the experimental results clearly demonstrated that the H_2 σ bond could be remarkably activated by some cooperative effect of multiple H_2 molecules interacting with the B^+ ion. To understand this observation more fully, we undertook a high-level ab initio electronic structure investigation

(1) Nichols, J.; Gutowski, M.; Cole, S. J.; Simons, J. *J. Phys. Chem.* **1992**, *96*, 644.
(2) Ruatta, S. A.; Hanley, L.; Anderson, S. L. *J. Chem. Phys.* **1989**, *91*, 226.
(3) Armentrout, P. B. *Int. Rev. Phys. Chem.* **1990**, *9*, 115.
(4) Lin, K. C.; Watkins, H. P.; Cotter, R. J.; Koski, W. S. *J. Chem. Phys.* **1974**, *60*, 5134.
(5) Kemper, P. R.; Bushnell, J. E.; Weis, P.; Bowers, M. T. *J. Am. Chem. Soc.* **1998**, *120*, xxxx.
(6) Bushnell, J. E.; Kemper, P. R.; Maitre, P.; Bowers, M. T. *J. Am. Chem. Soc.* **1994**, *116*, 9710.
(7) van Koppen, P. A. M.; Kemper, P. R.; Bushnell, J. E.; Bowers, M. T. *J. Am. Chem. Soc.* **1995**, *117*, 2098.

S0002-7863(98)00089-4 CCC: $15.00
Published on Web 07/10/1998

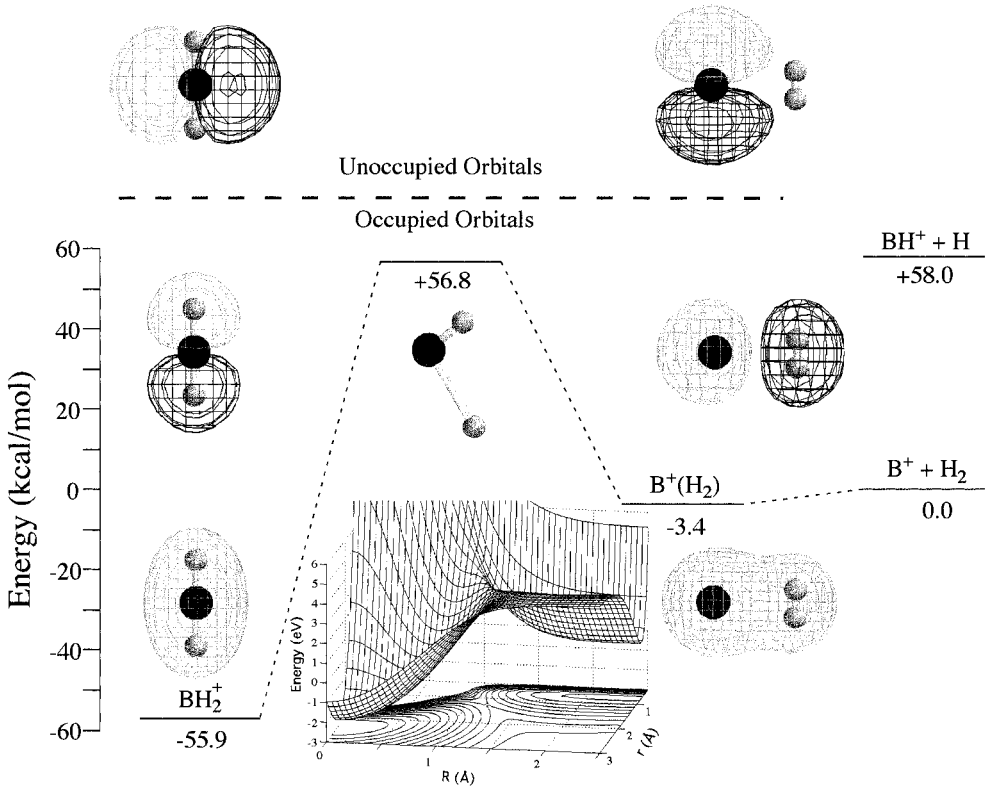

Figure 1. Relative energy of stationary points on the minimum energy path for $B^+ + H_2 \rightarrow BH_2^+$ calculated at the CCSD(T)/aug-cc-pVTZ level of theory with harmonic ZPE added for the *per*-hydrogenated species at the MP2/aug-cc-pVTZ level of theory. The transition state was calculated at the MRCISD/aug-cc-pVTZ level of theory. The orbitals pictured are the highest two occupied and lowest unoccupied valence orbitals for $B^+(H_2)$ and BH_2^+. The inset shows the potential energy surface for a constrained C_{2v} geometry.

of the series of reactions

$$B^+(H_2)_n + H_2 \rightarrow BH_2^+(H_2)_n \qquad (1)$$

for $n = 0-3$. In reaction 1, $B^+(H_2)_n$ denotes a cluster ion where the H_2 molecules are electrostatically bound to B^+ and $BH_2^+(H_2)_n$ denotes an ion where H_2 molecules are bound to the HBH^+ molecular ion.

Methods

All calculations were performed with the aug-cc-pVTZ basis set,[8,9] which is of triple-ζ quality augmented by diffuse functions. Inclusion of diffuse functions is particularly important for treating the electrostatic clusters because these functions are required to describe polarizability properly, which contributes significantly to the electrostatic bonding. For boron, the basis set consists of a (10s5p2d1f) set of primitive Gaussian functions contracted to [4s3p2d1f], which is augmented by an uncontracted (1s1p1d1f) set of diffuse functions. For hydrogen, the basis set consists of a (7s2p1d) set of primitive Gaussian functions contracted to [3s2p1d] and augmented by a (1s1p1d) set of diffuse functions. Pure spherical harmonic functions were used throughout.

Stationary points on the $B^+(H_2)_n$ and $BH_2^+(H_2)_{n-1}$ hypersurfaces were located and characterized with second-order Møller−Plesset (MP2) perturbation theory applied to a Hartree−Fock (HF) wave function with frozen core electrons. Analytical first derivatives were used to optimize geometric structures to a residual root-mean-square force of less than 10^{-6} hartree/bohr and analytical second derivatives were used to characterize a stationary point as a local minimum (all real harmonic frequencies) or a transition state (one imaginary harmonic frequency). For each transition state identified for these systems, the reaction coordinate was determined by displacing the geometry slightly in the direction of the eigenvector associated with the imaginary frequency (both positive and negative) and following the potential energy gradient to a subsequent stationary point on the potential energy surface.

An important exception to this approach was followed for the characterization of the transition state region for the B^+/H_2 system. Because this region of the potential energy surface is necessarily multiconfigurational, it could not be described well by MP2 calculations based on a single configuration HF wave function. Instead, complete active space (CAS) multiconfigurational self-consistent-field (MCSCF)[10,11] calculations followed by internally contracted configuration interaction in the single and double space (MRCISD)[12,13] were performed. In the MCSCF calculations the $(1s)^2$ electrons on boron were held frozen and the four valence electrons were distributed among the six orbitals arising from the 2s and 2p atomic orbitals of boron and the 1s atomic orbitals of each hydrogen atom.

At the stationary point geometries on the $B^+(H_2)_n$ and $BH_2^+(H_2)_{n-1}$ hypersurfaces identified by the MP2/aug-cc-pVTZ calculations, MRCISD and coupled cluster with single and double substitutions and a perturbative treatment of triple substitution (CCSD(T))[14] calculations were performed. (For H_2, CCSD calculations were performed instead because they correspond to full CI for a two-electron system.) These additional single-point calculations allowed two important issues to be addressed. First, a comparison of the CCSD(T) and MP2 results gave insight into the importance of electron correlation for describing correctly the relative energy of the various structures and bonding motifs because CCSD(T) captures more electron correlation than does MP2. And second, a comparison of the CCSD(T) and the MRCISD results gave insight into the validity of using single configurational approaches (i.e., MP2 and CCSD(T)) for geometries far from the B^+/H_2 transition state region.

(8) Dunning, T. H., Jr. *J. Chem. Phys.* **1989**, *90*, 1007.
(9) Kendal, R. A.; Dunning, T. H., Jr.; Harrison, R. J. *J. Chem. Phys.* **1992**, *96*, 6796.
(10) Werner, H.-J.; Knowles, P. J. *J. Chem. Phys.* **1985**, *82*, 5053.
(11) Knowles, P. J.; Werner, H.-J. *Chem. Phys. Lett.* **1985**, *115*, 259.
(12) Werner, H.-J.; Reinsch, E. A. *J. Chem. Phys.* **1988**, *89*, 5803.
(13) Knowles, P. J.; Werner, H.-J. *Chem. Phys. Lett.* **1988**, *145*, 514.
(14) Raghavachari, K.; Trucks, G. W.; Pople, J. A.; Head-Gordon, M. *Chem. Phys. Lett.* **1989**, *157*, 479.

Table 1. Calculated Energy and Geometry of the $B^+(^1S_g)$ with $H_2(^1\Sigma_g^+)$ Reactants

species	method[a]	energy (au)	r_{H_2} (Å)	ZPE(H) (cm^{-1})	ZPE(D) (cm^{-1})
B^+	MP2	−24.272821			
B^+	CCSD[b]	−24.296627			
H_2	MP2	−1.165023	0.73744	2258.8	1597.8
H_2	CCSD[b]	−1.172636	0.74298	2200.6	1556.6
H_2	expt[c]		0.74144	2200.6	1557.8
$B^+/3H_2$	MRCISD	−27.812429	0.74298[d]		
$B^+/3H_2$	MRCISD+Q	−27.816150	0.74298[d]		

[a] aug-cc-pVTZ basis set used throughout. [b] CCSD is exact for a two-electron system (i.e., H_2 and B^+ with frozen core electrons). [c] Huber, K. P.; Herzberg, G. *Constants of Diatomic Molecules*; Van Nostrand Reinhold: New York, 1979. [d] CCSD geometry was used.

The MP2 and CCSD(T) calculations were performed with the GAUSSIAN 94[15] suite of programs and the MRCISD calculations were performed with the MOLPRO[16] electronic structure package. All calculations were performed on a DEC alpha 3000/700 workstation.

Results

To facilitate comparisons between the properties of the various stationary points, only a subset of internal coordinates and harmonic vibrational frequencies will be reported here. A full description of the optimized geometries and vibrational frequencies will be provided as Supporting Information. The coordinates R, r_{H_2}, and θ_{R,rH_2} will be used to denote the distance between the boron atom and the midpoint of an H_2 molecule, the H_2 bond length, and the angle between R and r_{H_2}, respectively. The coordinates r_{BH} and θ_{HBH} will denote the BH bond length and HBH bond angle in the BH_2^+ moiety of a $BH_2^+(H_2)_{n-1}$, respectively. The angle formed by two different R coordinates will be denoted $\theta_{R,R'}$. The transition states which have been identified along the minimum energy pathway (MEP) connecting the reactants and products for these systems will be denoted TS_{ni}, where n indicates the number of H_2 molecules and i is an integer index. To further simplify comparisons, the electronic energy of $B^+(H_2)_n$ and $BH_2^+(H_2)_{n-1}$ and harmonic zero-point energies (ZPEs) are reported relative to the energies of the corresponding infinitely separated $B^+ + nH_2$ reactants. Unscaled harmonic frequencies are used in the calculation of ZPEs. The calculated properties of these reactants are summarized in Table 1. Because MP2 and CCSD(T) are size extensive, the electronic energy of multiple H_2 molecules is simply the corresponding multiple of the single H_2 molecule energy. Unfortunately, MRCISD calculations do not enjoy this property. Consequently, MRCISD energies can be compared properly only when the calculations consider the same number of H_2 molecules (i.e., the supermolecule approach), which was taken to be three in this study. Davidson[17] has proposed a correction (Q) to partially compensate for the size nonextensivity of MRCISD calculations and MRCISD+Q energies will also be reported as appropriate.

Table 2. Calculated Geometry and Relative Energy for $B^+(H_2)$ and BH_2^+ Stationary Points

property	electrostatic complex	hypersaddle point	transition state[a]	covalent molecular ion
point group	C_{2v}	C_{2v}	C_s	$D_{\infty h}$
R (Å)/MP2	2.2721			
R (Å)/CCSD(T)	2.2546			
R (Å)/MRCISD	2.2425	1.2056	2.7762	
r_{H_2} (Å)/MP2	0.7509			
r_{H_2} (Å)/CCSD(T)	0.7563			
r_{H_2} (Å)/MRCISD	0.7625	1.3348	2.4159	
r_{BH} (Å)/MP2				1.1702
r_{BH} (Å)/MRCISD			1.2079	1.1749
relative energy[b]				
MP2	−4.26			−64.46
CCSD(T)	−4.29			−60.57
MRCISD	−4.23	69.72	59.10	−60.39
MRCISD+Q	−4.40	69.94	59.06	−60.53
relative ZPE[c]				
per-H	0.92[d]		−2.27[e]	4.63[d]
per-D	0.68[d]		−1.50[e]	3.66[d]

[a] Angle between r_{H_2} and r_{BH} is 98.1°. [b] Relative to $B^+ + H_2$ in kcal/mol. [c] Relative to $H_2(D_2)$ in kcal/mol. [d] At the MP2/aug-cc-pVTZ level of theory. [e] At the MRCISD/aug-cc-pVTZ level of theory.

Inspection of Table 1 indicates that the CCSD/aug-cc-pVTZ calculations for H_2 give a bond length and harmonic frequency values that are in excellent agreement with experiment whereas the MP2 bond length and harmonic frequency are about 0.5% longer and 1.0% larger, respectively. Some insight into the effectiveness of the Davidson correction for this system can be obtained by comparing the MRCISD and MRCISD+Q energies with the CCSD energy of $B^+ + 3H_2$ because each of these species is an effective two-electron system (with the core electrons of B^+ frozen) and CCSD is exact for a true two-electron system. In this case, Q is less than 3 mHartrees and the CCSD energy falls almost midway between the MRCISD and MRCISD+Q results.

$B^+(H_2)$ and BH_2^+. Geometric and energetic parameters characterizing various stationary points on this hypersurface are summarized in Table 2. The electrostatic complex is calculated to be T-shaped (C_{2v}) with R equal to 2.27 (MP2), 2.25 (CCSD(T)), or 2.24 Å (MRCISD). The H_2 moiety is little changed from its infinitely separated characteristics with an r_{H_2} bond length that is increased only 0.013 (MP2 and CCSD(T)) or 0.020 Å (MRCISD) and a stretching frequency that is decreased by only 211.5 (MP2) or 197.3 cm^{-1} (CCSD(T)). The dissociation energies (D_e) calculated at the MP2, CCSD(T), and MRCISD levels of theory agree extremely well with each other, falling within the range of 4.26 ± 0.03 kcal/mol while the MRCISD+Q calculations predict a D_e about 0.14 kcal/mol larger. Inclusion of MP2 ZPE predicts adiabatic dissociation energies (D_0) which are decreased from the D_e value by 0.92 and 0.68 kcal/mol for the *per*-hydrogenated and *per*-deuterated species, respectively. To assess the adequacy of MP2 theory for predicting D_0, CCSD(T) harmonic frequencies were also calculated for the $B^+(H_2)$ electrostatic complex. The low-frequency modes of B^+- -H_2 stretching (345 cm^{-1}, MP2; 346 cm^{-1}, CCSD(T)) and H_2 rocking (511 cm^{-1}, MP2; 504 cm^{-1}, CCSD(T)) have very similar values at the two levels of theory while the high-frequency H_2 stretching mode (4306 cm^{-1}, MP2; 4204 cm^{-1}, CCSD(T)) appears to be overestimated by MP2 theory. However, the error is comparable to that observed for the isolated H_2 stretching frequencies (4518 cm^{-1}, MP2; 4401 cm^{-1}, CCSD),

(15) *Gaussian 94*, Revision B.3, Frisch, M. J.; Trucks, G. W.; Schlegel, H. B.; Gill, P. M. W.; Johnson, B. G.; Robb, M. A.; Cheeseman, J. R.; Keith, T.; Petersson, G. A.; Montgomery, J. A.; Raghavachari, K.; Al-Laham, M. A.; Zakrzewski, V. G.; Ortiz, J. V.; Foresman, J. B.; Peng, C. Y.; Ayala, P. Y.; Chen, W.; Wong, M. W.; Andres, J. L.; Replogle, E. S.; Gomperts, R.; Martin, R. L.; Fox, D. J.; Binkley, J. S.; Defrees, D. J.; Baker, J.; Stewart, J. P.; Head-Gordon, M.; Gonzalez, C.; Pople, J. A. Gaussian, Inc.: Pittsburgh, PA, 1995.

(16) MOLPRO is a package of ab initio programs written by Werner, H.-J.; Knowles, P. J. with contributions from Almlöf, J.; Amos, R. D.; Deegan, M. J. O.; Elbert, S. T.; Hampel, C.; Meyer, W.; Peterson, K.; Pitzer, R.; Stone, A. J.; Taylor, P. R.; Lindh, R.

(17) Langhoff, S. R.; Davidson, E. R. *Int. J. Quantum Chem.* **1974**, *8*, 61.

Table 3. Calculated Geometry[a] and Relative Energy for $B^+(H_2)_2$ and $BH_2^+(H_2)$ Stationary Points

property	electrostatic complex[b]	transition state 1	transition state 2	covalent molecular ion	transition state 3
point group	C_s	C_{2v}	C_{2v}	C_{2v}	D_{4h}
R (Å)	2.2511 (||) 2.2848 (⊥)	2.2636	1.5008	1.3699	0.8525
r_{H_2} (Å)	0.7509 (||) 0.7502 (⊥)	0.7506	0.8721	0.8103	1.7049
r_{BH} (Å)			1.4121	1.1729	1.2056
θ_{HBH} (deg)				141.2	
θ_{R,rH_2} (deg)	91.4 (||) 90.0 (⊥)	92.3	70.0	90.0	90.0
$\theta_{R,R'}$ (deg)	78.5	78.9	75.8		90.0
relative energy[c]					
MP2	−8.42	−8.33	0.06	−88.25	−57.71
CCSD(T)	−8.41	−8.33	3.51	−79.46	−50.54
MRCISD	−8.75		3.83	−79.12	−49.51
MRCISD+Q	−8.30		2.89	−79.53	−50.85
relative ZPE[d]					
per-H	2.35	2.14	4.68	9.86	5.57
per-D	1.72	1.58	3.49	7.47	4.38

[a] Geometry optimized at the MP2 level only. [b] (||) and (⊥) refer to the H_2 molecules which parallel and perpendicular to the plane of symmetry, respectively. [c] Relative to $B^+ + 2H_2$ in kcal/mol. [d] Relative to $2H_2(2D_2)$ in kcal/mol.

suggesting that harmonically based D_0 values can be adequately predicted for these systems by MP2 theory.

The covalently bound BH_2^+ molecule is calculated to be a linear symmetric molecule ($D_{\infty h}$) with an r_{BH} equal to 1.170 (MP2) or 1.175 Å (MRCISD). D_e values calculated at the CCSD(T), MRCISD, and MRCISD+Q levels of theory agree well with each other, falling in the range of 60.38 ± 0.09 kcal/mol, suggesting that the MP2 value may be about 4 kcal/mol too large. MP2 harmonic frequencies for the *per*-hydrogenated species are calculated to be 2729, 1009, and 3014 cm^{-1} for the symmetric stretching, bending, and asymmetric stretching modes, respectively. These results indicate that D_0 is decreased from D_e by 4.63 and 3.66 kcal/mol for the *per*-hydrogenated and *per*-deuterated species, respectively.

Two saddle points have been found on the $B^+(H_2)/BH_2^+$ hypersurface. The first has a C_{2v} geometric structure and corresponds to the second-order saddle point identified previously by the MCSCF calculations of Nichols et al. In that work the optimized geometry had $R = 1.226$ Å, $r_{H_2} = 1.396$ Å, and an energy of 77.6 kcal/mol with respect to $B^+ + H_2$. In the present MRCISD calculations this second-order saddle point is characterized by $R = 1.206$ Å, $r_{H_2} = 1.335$ Å, and an energy of 69.7 kcal/mol with respect to $B^+ + H_2$. The second saddle point has not been identified previously and represents the true transition state for this reaction. The geometric structure has C_s symmetry with the short $r_{BH} = 1.208$ Å, $r_{H_2} = 2.416$ Å, and $\theta_{BHH} = 98.1°$ (Figure 1). The hydrogen atoms are very inequivalent in this transition state with the long $r_{BH} = 2.849$ Å. Inclusion of ZPE decreases the transition state energy by 2.27 and 1.50 kcal/mol for the *per*-hydrogenated and *per*-deuterated species, respectively. The relative energy of the stationary points along the MEP is summarized in Figure 1.

$B^+(H_2)_2$ and $BH_2^+(H_2)$. Geometric and energetic parameters characterizing various stationary points on this hypersurface are summarized in Table 3 and illustrated in Figure 2. The electrostatic complex is calculated at the MP2 level to have a C_s minimum energy structure with the values of R and r_{H_2} comparable to those of the $B^+(H_2)$ electrostatic complex. Each H_2 adopts a T- or near-T-shaped structure with the B^+ ion with $\theta_{R,R'}$ equal to 78.5°. All of the methods investigated predict very similar values for the D_e of this complex to $B^+ + 2H_2$ which fall in the range of 8.53 ± 0.23 kcal/mol. Lying only about 0.1 kcal/mol in energy above this structure is a planar C_{2v} transition state, TS_{21}. Interestingly, Table 3 indicates that, when harmonic ZPE is considered, TS_{21} is about 0.5 kcal/mol more stable than the C_s minimum. This result suggests that the electrostatic complex may be a very fluxional molecule without a well-defined equilibrium geometry.

Continuing along the MEP from TS_{21} brings the system to TS_{22}, which is the true transition state for the reaction. The major geometric changes between TS_{21} and TS_{22} are a shortening of R by about 0.76 Å and an elongation of r_{H_2} by about 0.12 Å. TS_{22} is a planar five-member ring from which the covalent molecular ion is formed through a pericyclic mechanism where simultaneously two BH bonds are formed, two H_2 bonds are broken, and a new H_2 bond is formed. It is worth emphasizing that this mechanism implies that the two hydrogen atoms that ultimately participate in the two BH bonds of $BH_2^+(H_2)$ originate from different hydrogen molecules as do the two hydrogen atoms which ultimately form the H_2. The final transition state considered for this system, TS_{23}, can internally exchange the hydrogens involved in the BH bonds in the covalent molecular ion with those involved in the H_2 bonding. TS_{23} has a square-planar geometry (D_{4h}) with four equivalent hydrogens. However, the energy of TS_{23} lies above that of $BH_2^+ + H_2$, indicating that dissociation is energetically preferred over internal hydrogen exchange through this transition state.

$B^+(H_2)_3$ and $BH_2^+(H_2)_2$. Geometric and energetic parameters characterizing various stationary points on this hypersurface are summarized in Table 4 and illustrated in Figure 3. The electrostatic complex is calculated at the MP2 level to have a C_3 minimum energy structure with the values of R and r_{H_2} comparable to those of the $B^+(H_2)$ and $B^+(H_2)_2$ electrostatic complexes. Again, each H_2 adopts a near-T-shaped structure with the B^+ ion with $\theta_{R,R'}$ equal to about 78°. All of the methods investigated predict very similar values for the D_e of this complex to $B^+ + 3H_2$ which fall in the range of 12.51 ± 0.35 kcal/mol. The structure of the transition state for forming the covalent molecular ion, TS_{31}, is very similar to the that of electrostatic complex with the most significant geometric changes occurring in coordinates of θ_{R,rH_2} and R which decrease by about 20° and 0.43 Å, respectively. Because these motions of the H_2 molecules are associated with a small energy change, the electronic surface at TS_{31} is only about 3.4 kcal/mol higher

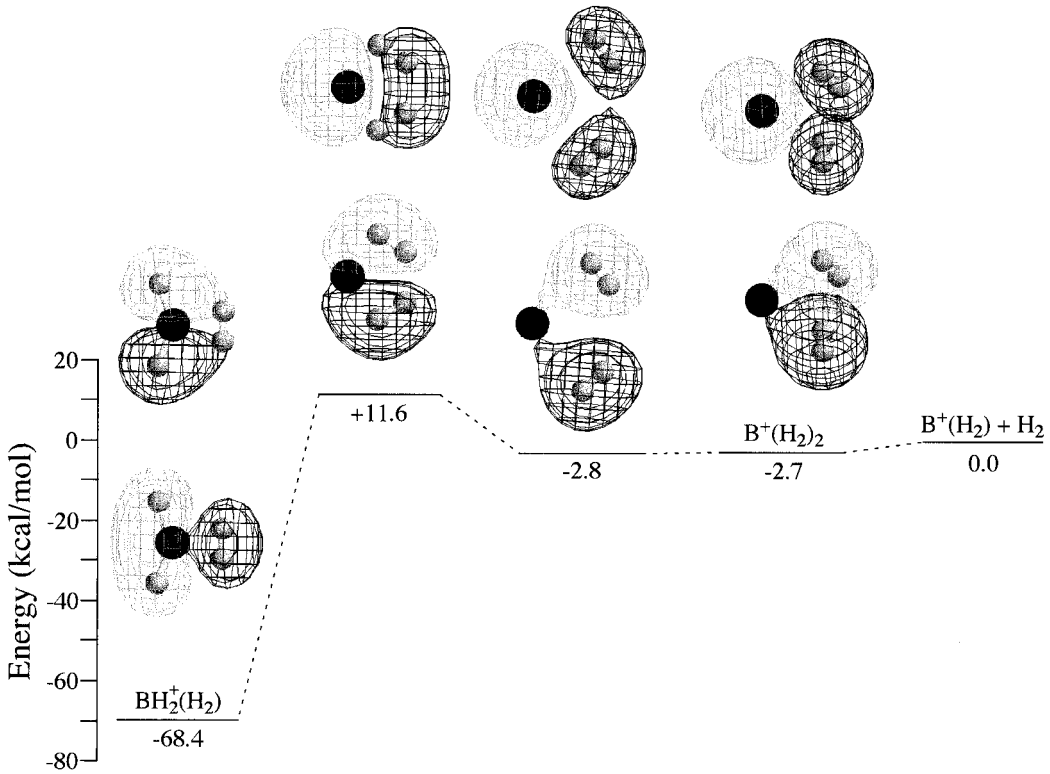

Figure 2. Relative energy of stationary points on the minimum energy path for $B^+(H_2) + H_2 \rightarrow BH_2^+(H_2)$ calculated at the CCSD(T)/aug-cc-pVTZ level of theory with harmonic ZPE added for the *per*-hydrogenated species at the MP2/aug-cc-pVTZ level of theory. The orbitals pictured show the evolution of the highest two occupied valence orbitals along the reaction path.

Table 4. Calculated Geometry[a] and Relative Energy for $B^+(H_2)_3$ and $BH_2^+(H_2)_2$ Stationary Points

property	electrostatic complex	transition state 1	transition state 2	covalent molecular ion
point group	C_3	C_{3v}	D_{3h}	C_{2v}
R (Å)	2.2418	1.8089	1.1027	1.3123
r_{H_2} (Å)	0.7509	0.7759	1.0694	0.8196
r_{BH} (Å)			1.2255	1.1810
θ_{HBH} (deg)			51.7	123.0
θ_{R,rH_2} (deg)	92.2	70.6	90.0	90.0
$\theta_{R,R'}$ (deg)	77.9	77.4	120.0	100.1
relative energy[b]				
MP2	−12.66	−10.27	−89.18	−111.57
CCSD(T)	−12.51	−9.08	−78.69	−102.28
MRCISD	−12.86	−9.14		−101.67
MRCISD+Q	−12.16	−9.07		−101.95
relative ZPE[c]				
per-H	4.26	6.42	12.64	16.23
per-D	3.11	4.70	9.60	12.11

[a] Geometry optimized at the MP2 level only. [b] Relative to $B^+ + 3H_2$ in kcal/mol. [c] Relative to $3H_2(3D_2)$ in kcal/mol.

in energy than the electrostatic minimum. From TS_{31} the MEP leads to TS_{32}, a high-symmetry (D_{3h}) transition state where the B^+ ion interacts equivalently with all six hydrogens. At this point on the MEP nearly 75% of the reaction exothermicity has been released. From TS_{32}, motion along the MEP involves an asymmetric distortion that breaks the C_3 symmetry which has been preserved thus far, leading the system to the covalent molecular ion.

$B^+(H_2)_4$ and $BH_2^+(H_2)_3$. Geometric and energetic parameters characterizing various stationary points on this hypersurface are summarized in Table 5. The $B^+(H_2)_4$ electrostatic complex is calculated at the MP2 level to have a C_s minimum energy structure with the values of R and r_{H_2} comparable to those of the other electrostatic complexes and with each H_2 adopting a T- or near-T-shaped structure with the B^+ ion. The symmetry plane contains one H_2 and bisects a second H_2, which have a $\theta_{R,R'}$ equal to about 78° with respect to each other. The other two H_2 lie in equivalent positions on either side of the symmetry plane having a $\theta_{R,R'}$ of about 77−78° with respect to the first two H_2 molecules and a $\theta_{R,R'}$ of about 147° with respect to each other. CCSD(T) and MP2 calculations predict similar values of about 15.46 ± 0.06 kcal/mol for the D_e of this complex to $B^+ + 4H_2$. The transition state for forming the covalent molecular ion (TS_{41}) has C_s symmetry (although a plane of symmetry is not preserved in going from the electrostatic complex to TS_{41}) and is very similar to TS_{31} with the additional H_2 located far from the B^+ ion (R = 2.82 Å). From TS_{41}, the MEP proceeds to the covalent molecular ion that is structurally very similar to that of $BH_2^+(H_2)_2$ with an additional weakly bound H_2 molecule. Two different local minima for the location of this final H_2 were found. One is a C_s structure where the weakly bound H_2 molecule is located between the covalently bound H_2 molecules but much further away from the B^+ ion. The other is a C_1 structure where the weakly bound H_2 molecule is located about midway between the plane of boron and one covalently bound H_2 and the BH_2^+ plane. These two minima and the transition state connecting them (TS_{42}) all lie within about 1 kcal/mol of each other.

Discussion

Although the results were presented with each system distinguished by the number of H_2 molecules present, instructive trends in the results can be identified best by regrouping the systems under the headings of electrostatic complexes, covalent molecular ions, and the intervening transition states. It is also instructive to consider the relative energetics for the stepwise addition of each H_2 molecule within each of these groups. Although this information is implicit in Tables 2−5, it is

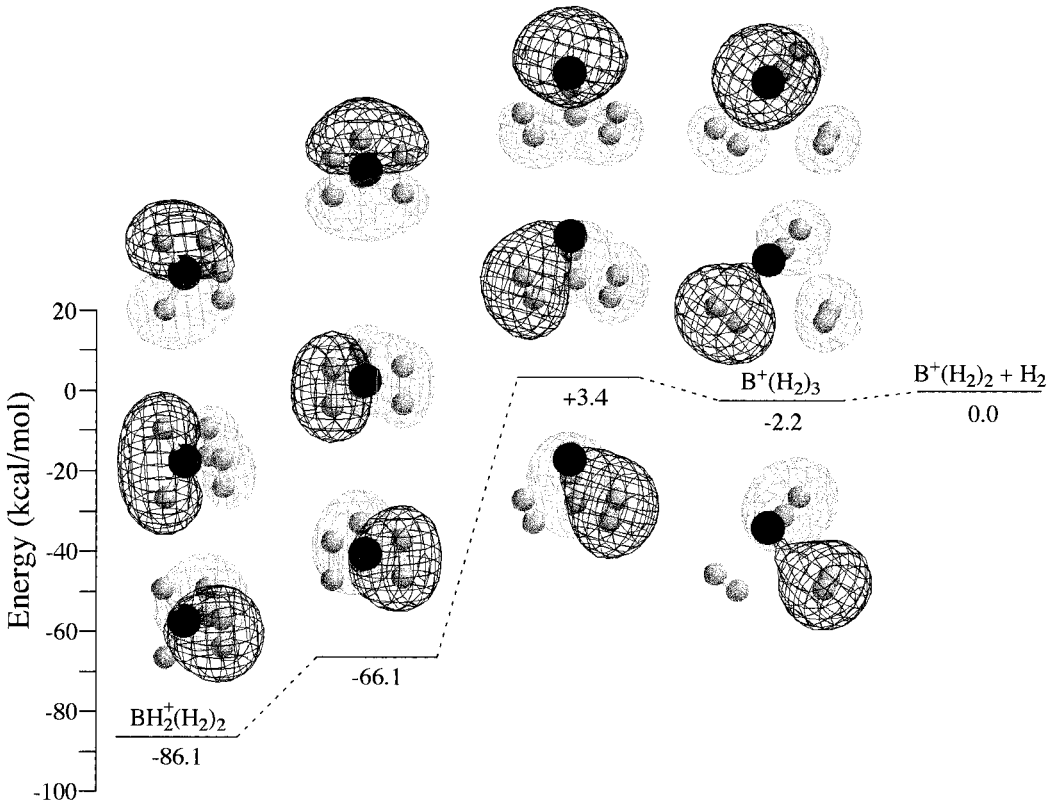

Figure 3. Relative energy of stationary points on the minimum energy path for $B^+(H_2)_2 + H_2 \rightarrow BH_2^+(H_2)_2$ calculated at the CCSD(T)/aug-cc-pVTZ level of theory with harmonic ZPE added for the *per*-hydrogenated species at the MP2/aug-cc-pVTZ level of theory. The orbitals pictured show the evolution of the highest three occupied valence orbitals along the reaction path.

Table 5. Calculated Geometry[a] and Relative Energy for $B^+(H_2)_4$ and $BH_2^+(H_2)_3$ Stationary Points

property	electrostatic complex	transition state 1	covalent molecular ion 1	transition state 2	covalent molecular ion 2
point group	C_s	C_s	C_s	C_s	C_1
R (Å)	2.2157	1.8166	1.3121	1.3052	1.3155
	2.2416	1.8166	1.3121	1.3115	1.3531
	2.4391	1.8815	3.1901	3.7715	3.1090
	2.4391	2.8156			
r_{H_2} (Å)	0.7513	0.7780	0.8191	0.8189	0.8181
	0.7506	0.7780	0.8191	0.8197	
	0.7461	0.7726	0.7414	0.7403	0.7401
	0.7461	0.7419			
r_{BH} (Å)			1.1806	1.1811	1.1809
			1.1809	1.1811	1.1809
θ_{HBH} (deg)			123.1	122.6	123.0
θ_{R,rH_2} (deg)	90.0	71.2	89.8	90.0	90.0
	92.4	71.2	89.8	90.0	89.9
	91.8	70.5	82.7	90.0	99.9
	91.8	76.5			
$\theta_{R,R'}$ (deg)	77.7	78.0	99.6	100.3	99.7
	76.8	78.1	59.6	0.0	156.3
	76.8	72.9	59.6	100.3	57.3
	77.9	78.1			
	77.9	72.9			
	147.4	139.0			
relative energy[b]					
MP2	−15.52	−12.33	−113.78	−113.17	−113.21
CCSD(T)	−15.40	−11.05	−104.52	−103.91	−103.95
relative ZPE[c]					
per-H	5.58	7.84	17.68	17.24	17.25
per-D	4.09	5.72	13.14	12.83	12.83

[a] Geometry optimized at the MP2 level only. R, r_{H_2}, and θ_{R,rH_2} values correspond to the same H_2 molecule in the order listed. $\theta_{R,R'}$ values corespond to the angle between the first and second H_2 listed, followed by the first and third, and so on until the third and fourth. [b] Relative to $B^+ + 3H_2$ in kcal/mol. [c] Relative to $3H_2(3D_2)$ in kcal/mol.

summarized in Table 6 for convenience. To produce a consistent set of energy differences, CCSD(T) electronic energies and MP2 ZPEs were used generally because the CCSD(T) and the MRCISD results are in good agreement and CCSD(T) values are available for all systems considered. An important exception is the $(BH_2^+)^\dagger$ transition state, which requires a

Table 6. Calculated Energy Changes (kcal/mol) for the Indicated Reactions

reaction	electronic	*per*-H_2	*per*-D_2
	Electrostatic Complex Formation		
$B^+ + H_2 \rightarrow B^+(H_2)$	−4.3	−3.4 (−3.8 ± 0.2)[a]	−3.6
$B^+(H_2) + H_2 \rightarrow B^+(H_2)_2$	−4.1	−2.7 (−3.0 ± 0.3)[a]	−3.1
$B^+(H_2)_2 + H_2 \rightarrow B^+(H_2)_3$	−4.1	−2.2	−2.7
$B^+(H_2)_3 + H_2 \rightarrow B^+(H_2)_4$	−2.9	−1.6	−1.9
$BH_2^+(H_2)_2 + H_2 \rightarrow BH_2^+(H_2)_2(H_2)$	−2.2	−0.8	−1.2
	Covalent Bond Formation		
$B^+ + H_2 \rightarrow BH^+ + H$	+61.8	+58.0	+58.9
$B^+ + H_2 \rightarrow BH_2^+$	−60.6	−55.9	−56.9
$BH_2^+ + H_2 \rightarrow BH_2^+(H_2)$	−18.9	−13.7 (−14.7 ± 0.5)[a]	−15.1
$BH_2^+(H_2) + H_2 \rightarrow BH_2^+(H_2)_2$	−22.8	−16.5 (−18.1 ± 0.5)[a]	−18.2
	Transition State Formation		
$B^+ + H_2 \rightarrow (BH_2^+)^\dagger$	+59.1	+56.8	+57.6
$B^+(H_2) + H_2 \rightarrow (B^+(H_2)_2)^\dagger$	+7.8	+11.6	+10.6
$B^+(H_2)_2 + H_2 \rightarrow (B^+(H_2)_3)^\dagger$	−0.7	+3.4	+2.3
$B^+(H_2)_3 + H_2 \rightarrow (B^+(H_2)_4)^\dagger$	+1.5	+5.0	+4.1

[a] Experimental values from ref 5.

multireference technique for a correct description and MRCISD electronic energy, and harmonic frequencies are used in this case.

Electrostatic Complex Formation. Each H_2 molecule in every electrostatic complex investigated adopts a T- or near-T-shaped orientation ($\theta_{R,rH_2} \sim 90°$), which is the attractive orientation of the H_2 quadrupole moment with a positive charge. The position of H_2 molecules with respect to each other is also consistent, maintaining a $\theta_{R,R'}$ value of about 78°. Noting that this value of $\theta_{R,R'}$ is close to the mutual angle between the three empty p-orbitals of B^+ (i.e., 90°) suggests that these empty orbitals are instrumental in transferring electron density from the H_2 molecules to the B^+ ion. The structures of the $B^+(H_2)_2$ and $B^+(H_2)_3$ complexes indicate a preference for each p-orbital to interact with a single H_2 molecule, and the similarity of the electronic binding energy of the first three H_2 molecules (4.3, 4.1, and 4.1 kcal/mol) indicates that each of these sequential binding events are largely independent from a electronic point of view. Formation of $B^+(H_2)_4$ requires that two H_2 molecules interact with the same p-orbital and Table 6 indicates that this requirement causes a ~30% decrease in the electronic binding energy. The structure of $B^+(H_2)_4$ indicates a preference for the H_2 molecules to be on the "same side" of the B^+ with all $\theta_{R,R'}$ values (except that involving the two H_2 molecules interacting with the same p-orbital) being 77.4 ± 0.6°.

The present adiabatic electrostatic binding energies for the *per*-hydrogenated clusters can be compared with the QCISD(T)/6-311++G(2df,p) computational and clustering equilibrium experimental results of KBWB. Computationally, the present binding energies are about 10% larger for $B^+(H_2)$ and $B^+(H_2)_2$ formation (3.4 kcal/mol vs 3.1 kcal/mol and 2.7 kcal/mol vs 2.5 kcal/mol, respectively) and about 10% smaller for $B^+(H_2)_3$ and $B^+(H_2)_4$ formation (2.2 kcal/mol vs 2.3 kcal/mol and 1.6 kcal/mol vs 1.9 kcal/mol, respectively). Ordinarily, QCISD(T) and CCSD(T) calculations with comparable basis sets would be expected to give very similar results. It is possible that the small discrepancies in computed binding energies arise from the present use of MP2 ZPEs and the KBWB use of SCF ZPEs. The binding energies for $B^+(H_2)$ and $B^+(H_2)_2$ formation presently calculated are in better agreement with the experimental values (3.8 ± 0.2 and 3.0 ± 0.3 kcal/mol, respectively) than are the calculations of KBWB.

The results in Tables 5 and 6 indicate that the covalently bound $BH_2^+(H_2)_3$ is best considered as an electrostatic complex between $BH_2^+(H_2)_2$ and H_2 and is thus denoted $BH_2^+(H_2)_2(H_2)$ in Table 6. The electrostatic binding of the first H_2 to $BH_2^+(H_2)_2$ is weaker than the electrostatic binding of the fourth H_2 to B^+, suggesting that the $B^+(H_2)_4$ complex is more likely to be observed mass spectrometrically despite having an overall stability that is much less than that of the isomeric cluster, $BH_2^+(H_2)_2(H_2)$. This result can be rationalized by considering the size difference between $BH_2^+(H_2)_2$ and B^+, which causes the electrostatically bound H_2 molecule in $BH_2^+(H_2)_2(H_2)$ to be about 1 Å further from the boron atom than it is in the $B^+(H_2)_4$ complex.

Covalent Bond Formation. The reaction of $B^+ + H_2$ to form BH_2^+ is calculated to be about 56.8 kcal/mol exothermic, which agrees well with the QCISD(T) result of 55.7 kcal/mol calculated by KBWB but is substantially greater than the MCSCF of 42.1 kcal/mol reported by Nichols et al. However, building CI on to the multireference wave function, as is done in the MRCISD calculations, repairs this deficiency of the MCSCF calculations.

Binding of an H_2 molecule to BH_2^+ is calculated to be exothermic by 13.7 kcal/mol, which agrees well with the computational (13.8 kcal/mol) and experimental (14.7 ± 0.5 kcal/mol) results of KBWB as well as with the MP2(fu)/6-311G(d,p) calculations (14.5 kcal/mol) of DePuy *et al.*[18] The latter agreement is surprising considering that the present MP2 and CCSD(T) results differ by almost 5 kcal/mol for the exothermicity of this reaction. It is possible that the near agreement with the results of DePuy et al. may be due to their use of a somewhat smaller basis set and/or the correlation of the 1s electrons of boron. Technical comparisons aside, however, it is clear that the binding energy of H_2 to BH_2^+ is about 5 times greater than is the binding of H_2 to $B^+(H_2)$. Coupling this energetic result with the geometric results of a long H_2 bond (0.81 Å vs 0.75 Å) and short value of R (1.37 vs 2.25 Å) in $BH_2^+(H_2)$, relative to the value of those parameters in $B^+(H_2)_2$, indicates a significant degree of covalent character in the bonding of H_2 to BH_2^+. This was first noted by Rasul and Olah,[19] who pointed out the three center-two electron (3c−2e) nature of this bonding. This bonding picture of boron participating in one 3c−2e bond with the H_2 species and two 2c−2e bonds in the BH_2^+ moiety is supported by the θ_{HBH} angle of 141.2°, which is close to the 120° angle expected for three pairs of electrons around a central atom. Further, a comparison of the vibrational frequencies indicates that the formation of the 3c−2e bond seems to have little effect on the 2c−2e bonding

(18) DePuy, C. H.; Gareyev, R.; Hankin, J.; Davico, G. E. *J. Am. Chem. Soc.* **1997**, *119*, 427.
(19) Rasul, G.; Olah, G. A. *Inorg. Chem.* **1997**, *36*, 1278.

in the BH_2^+ moiety beyond the near 40° decrease in θ_{HBH}. The frequency of the symmetric stretch, in-plane bend, and asymmetric stretch of the BH_2^+ moiety in $BH_2^+(H_2)$ and the change from the corresponding value in BH_2^+ (in parentheses) are calculated to be 2734.2 (+5.3 cm^{-1}), 987.2 (−21.3 cm^{-1}), and 2939.1 cm^{-1} (−75.2 cm^{-1}). In contrast, the H_2 vibrational frequency decreases 938.3 cm^{-1} to 3579.3 cm^{-1} upon forming the 3c−2e bond.

Binding of the second H_2 to BH_2^+ is calculated to be about 3 kcal/mol more exothermic than the binding of the first H_2 in agreement with the computational and experimental results of KBWB and the computational results of DePuy et al. This increased exothermicity coupled with a long H_2 bond and short value of R similar to that observed for $BH_2^+(H_2)$ supports the bonding picture of a second 3c−2e bond formation as suggested by Rasul and Olah. This viewpoint gains further support when it is recognized that the two 2c−2e bonds and the two 3c−2e bonds form near-tetrahedral angles with respect to each other as expected for four pairs of electrons around a central atom. Again, a consideration of the vibrational frequencies indicates that the dominant effect of the formation of the two 3c−2e bonds on 2c−2e bonding in the BH_2^+ is the decrease in θ_{HBH}. In this case, the frequencies of the symmetric stretch, in-plane bend, and asymmetric stretch of the BH_2^+ moiety in $BH_2^+(H_2)_2$ and the change from the corresponding value in BH_2^+ (in parentheses) are calculated to be 2688.0 (−40.9 cm^{-1}), 1085.1 (+76.6 cm^{-1}), and 2813.8 cm^{-1} (−200.5 cm^{-1}), whereas the H_2 in-phase and out-of-phase stretching frequencies decrease to an average value of 3454.2 cm^{-1} (−1063.4 cm^{-1}).

Transition State Formation. The transition state for BH_2^+ formation from $B^+ + H_2$ is calculated to be about 57 kcal/mol, which is only about 1 kcal/mol less than the energy required to form $BH^+ + H$. This result coupled with the calculated transition state structure of an essentially fully formed BH bond (r_{BH} = 1.208 Å, identical to the equilibrium bond length of BH^+), and an essentially fully dissociated H_2 bond (r_{H_2} = 2.416 Å), supports the mechanistic interpretation of sequential bond formation for this reaction. Although the origin of this activation has been discussed in detail in the Introduction, anticipating the results for reactions with additional H_2 molecules present, we offer the following perspective. To activate the H_2 for insertion, electron density needs to be shifted into an orbital having a node that bisects the H_2 bond. In the $B^+ + H_2$ reaction, this requires substantial rotation of the H_2 molecule (θ_{BHH} = 98.1° at the transition state) causing the B^+ ion to interact strongly with only one hydrogen of the H_2 molecule. Thus, the full energy price of breaking the H_2 bond must be paid while the pay back of forming only one of the two BH bonds is received. It can be anticipated that a substantial reduction in activation energy may ensue if the system can maneuver the node of an occupied molecular orbital to bisect an H_2 bond while allowing the B^+ ion to interact with multiple hydrogens.

This is precisely what occurs in the transition state for the reaction of $B^+(H_2) + H_2$ where the activation energy is lowered by nearly 80% to only about 11 kcal/mol. Figure 2 shows that this is accomplished by having the node in the HOMO, which lies between the B^+ ion and the two H_2 molecules in the electrostatic complex, shift at the transition state to where it begins to bisect both H_2 bonds while two bond-like BH distances (r_{BH} = 1.41 Å) are maintained. As mentioned previously, passing out of this transition state the system breaks two H_2 bonds while simultaneously forming two BH bonds and one new H_2 bond. As the system proceeds toward the $BH_2^+(H_2)$ product, the highest two occupied molecular orbitals exchange their relative energy ordering.

This strategy for activation energy reduction is used to greater advantage in the reaction of $B^+(H_2)_2 + H_2$ where more than 70% of the remaining activation energy is removed. Figure 3 shows that the relevant molecular orbital node is again that of the HOMO, which shifts at the transition state to begin to bisect all three H_2 bonds. In this transition state, the angle that the hydrogen atoms closest to boron make with boron ($\theta_{HBH'}$) is 95.2°. This angle suggests the hydrogen atoms nearest boron are strongly interacting with the three previously unoccupied p-orbitals of B^+ ion. Use of these orbitals will be crucial in formation of the ensuing two 2c−2e and two 3c−2e bonds. For this reaction path, the relative energy ordering of the molecular orbitals is preserved and only one H_2 bond is broken while two BH bonds are formed. Of the three detailed reaction mechanisms considered thus far, only this final one can be considered properly as an insertion mechanism.

The activation energy for the reaction of $B^+(H_2)_3 + H_2$ increases about 1.7 kcal/mol over that for the $B^+(H_2)_2 + H_2$ reaction, indicating that, for these systems, activation energy lowering by interacting with increasing numbers of H_2 molecules maximizes with three H_2 molecules. This value of three appears to be intimately associated with the fact that the B^+ ion has three empty p-orbitals. At the transition state for $B^+(H_2)_3 + H_2$ reaction, θ_{HBH} values for the three hydrogen atoms closest to B^+ are 95.0−96.3°, similar to the value observed for the $B^+(H_2)_2 + H_2$ transition state. However, R for one of these H_2 molecules is about 0.07 Å longer than the corresponding value in the $B^+(H_2)_2 + H_2$ transition state. This H_2 molecule is precisely the one that "shares" a B^+ p-orbital with another H_2 that moves far from the B^+ ion (R = 2.82 Å) at the transition state as if to leave as much of the p-orbital interaction for the H_2 that will participate significantly in the reaction. Because all other structural parameters characterizing $(B^+(H_2)_3)^\dagger$ and $(B^+(H_2)_4)^\dagger$ are so similar, it appears that the 1.7 kcal/mol increase in activation energy occurring with the addition of a fourth H_2 molecule arises from the necessity of sharing a B^+ p-orbital by two H_2 molecules. This interpretation suggests that no further reduction in activation energy is expected with participation of increasing numbers of H_2 molecules beyond three. Rather, a small increase in activation energy may continue to occur instead.

Comparison with Experiment. From an analysis of the temperature dependence of the rate of $BH_2^+(H_2)_2$ formation, KBWB inferred that the reactive species was $B^+(H_2)_3$ and that the barrier to reaction was 1.0 ± 0.5 kcal/mol. From a similar analysis of analogous experiments with deuterium substitution, a reaction barrier of 1.7 kcal/mol was inferred for the formation of $BD_2^+(D_2)_2$. The present computational results are in full agreement with the conclusion that $B^+(H_2)_3$ is the most reactive electrostatic complex. However, there are two major difficulties in interpreting the experimentally determined activation energies as classical adiabatic barriers to reaction. First, the kinetic analysis used by KBWB implies that the inferred activation energies are to be measured from the zero-point level of the respective electrostatic complex, placing the barriers 0.6 ± 0.5 and 0.2 kcal/mol below the energy of $B^+(H_2)_2 + H_2$ and $B^+(D_2)_2 + D_2$, respectively. Considering that these dissociation limits are the experimental starting points for complex formation, it is difficult to understand why production of the covalent molecular ion would be slow (as inferred in the experimental work) when reactants with zero relative kinetic energy have sufficient energy to undergo the reaction. It is conceivable that

the reaction rate may be slowed by a dynamical constraint that limits access to the transition state region and some evidence for the "tightness" of the transition state can be inferred from the increased ZPE of $(B^+(H_2)_3)^\dagger$ relative to that of $B^+(H_2)_3$. However, if the reactants did contain energy in excess of the classical adiabatic barrier, the reaction would ordinarily be thought to be facile under the experimental conditions of KBWB.

The second difficulty concerns the isotope effect on the activation energy. KBWB inferred a barrier height for the deuterated reaction which was greater than that for the hydrogenated reaction. Alternatively, the present computational results predict classical adiabatic reaction barriers of 3.4 and 2.3 kcal/mol for hydrogenated and deuterated reactants, respectively, if measured from the separated reactants. These barriers become 5.6 and 5.0 kcal/mol, respectively, if measured from the ZPE of the respective electrostatic complex. From either point of view, the classical adiabatic reaction barrier is predicted to decrease upon deuteration and this is a robust result of these calculations. Although it is true that the molecular hydrogen stretching frequencies are decreased at the transition state relative to their values in the electrostatic complex or separated reactants, this effect, which by itself would cause an increase in the adiabatic barrier upon deuteration, is more than offset by two additional considerations. First, at the transition state, the low-frequency modes of molecular hydrogen in the electrostatic complexes shift to higher energy as the strong bonding of the covalent molecular ion starts to develop. Second, with respect to the separated reactants, the transition state has five additional vibrational modes, all of which shift to lower frequency upon deuteration.

If the experimentally determined activation energies are not readily interpreted as classical adiabatic barrier heights, how should they be understood? One possibility is that they represent effective dynamical barrier heights. The effective mass associated with motion over the col at the transition state is calculated to be 1.1841 amu for $(B^+(H_2)_3)^\dagger$ and 2.4844 amu for $(B^+(D_2)_3)^\dagger$. These effective masses are light enough for tunneling at energies below the classical adiabatic barrier to contribute to the overall observed rate. Considering that the present calculations predict classical adiabatic reaction barriers which are a few kilocalories per mole above the dissociation energy of the electrostatic complexes, it is possible that the reaction mechanism may be dominated by tunneling under the experimental conditions of KBWB. If this is true, the experimental determination of an effective dynamical barrier that increases upon deuteration can be understood generally as a consequence of the greater effective mass of the deuterated reactants which decreases the tunneling rate relative to that of the hydrogenated reactants at the same energy above their respective ZPE.

One final mechanistic point can be noted. Because under the experimental conditions of KBWB electrostatic complexes are produced by a three-body association reaction,

$$(B^+(H_2)_2)^* + H_2 \rightarrow B^+(H_2)_2 + H_2 \qquad (2a)$$

where $(B^+(H_2)_2)^*$ is a collision complex, it might be thought that the required activation energy could be supplied as internal energy in $(B^+(H_2)_2)^*$. In this mechanism, the rate of covalent molecular ion formation would depend on the competition between reactions 2a and

$$(B^+(H_2)_2)^* + H_2 \rightarrow BH_2^+(H_2)_2 \qquad (2b)$$

However, the present calculations indicate that a fully energized $(B^+(H_2)_2)^*$ collision complex (i.e., having an energy equal to the dissociation energy) still requires an additional 0.71 kcal/mol to surmount the classical adiabatic reaction barrier. Interestingly, when the analogous *per*-deuterated reaction is considered, the calculations predict that the fully energized $(B^+(D_2)_2)^*$ collision complex has 0.77 kcal/mol in excess of its classical adiabatic reaction barrier. Thus if internal energy in the collision complexes played a significant role in promoting the reaction, the calculations indicate that the deuterated reaction should be favored. Experimentally, this is not the case.

Acknowledgment. We thank Professor Bowers for suggesting this investigation and for communicating his results in advance of publication. Acknowledgment is also made to NSF (CHE95-51008), the Robert A. Welch Foundation, and the Petroleum Research fund, administered by the American Chemical Society (PRF No. 28190-AC6), for partial support of this work.

Supporting Information Available: Tables giving the geometries of various $B^+(H_2)_n$ and $B^+(H_2)_{n-1}$ stationary points optimized at the MP2/ang-cc-pVTZ level of theory (11 pages, print/PDF). See any current masthead page for ordering information and Web access instructions.

JA980089X